Desalination and Water Treatment
www.deswater.com
doi: 10.5004/dwt.2020.26473

208 (2020) 355–366
December

Ionic liquid modified magnetic nanoparticles-graphene hybrid (Fe_3O_4@GO-IL) for the removal of ibuprofen and penicillin G from aqueous solutions

Bahareh Karimi[a], Leila Ma'mani[b,†], Abdulfattah Ahmad Amin[c], Hazhir Karimi[d], Hooshyar Hossini[e,*]

[a]*Environment and Energy Department, Islamic Azad University, Tehran, Iran, email: baharkarimi21@yahoo.com (B. Karimi)*
[b]*Department of Nanotechnology, Agricultural Biotechnology Research Institute of Iran (ABRII), Agricultural Research, Education and Extension Organization (AREEO), Karaj, Iran, Tel. +9826-32703536; email: l.mamani@abrii.ac.ir (L. Ma'mani)*
[c]*Department of Road Construction, Polytechnic University, Erbil Technology Institute, Erbil, Iraq, email: abdulfattah14ahmad@yahoo.com (A.A. Amin)*
[d]*Department of Environmental Science, Faculty of Science, University of Zakho, Kurdistan Region, Iraq, email: hazhir.karimi25@gmail.com (H. Karimi)*
[e]*Department of Environmental Health Engineering, Faculty of Health, Kermanshah University of Medical Sciences, Kermanshah, Iran, Tel. +98 9188594084; email: hoo.hosseini@gmail.com (H. Hossini)*

Received 12 October 2019; Accepted 19 August 2020

ABSTRACT

Pharmaceutical compounds with a toxic nature are released into the aquatic environment and can lead to adverse effects on ecological sustainability. Thus, enhancing the separation and treatment of the toxic compounds seem necessary. In this study, uptake and removal efficiency for the adsorption of two pharmaceutical compounds, ibuprofen (IBU) and penicillin G (PEN G), from aqueous solutions by Fe_3O_4@GO-IL were investigated. However, the effect of main effective variables including pH, concentrations, adsorbent dosage, and contact time were investigated. Isotherm and kinetic models also were studied. The maximum IBU removal rate was achieved about 97.58 (~5 mg/g) under optimal condition, pH 6.5, adsorbent dose 0.120 g/L, contact time 60 min, initial concentration 12.7 mg/L. At a condition of pH 4, adsorbent dose 0.3 g/L, contact time 97.5 min, initial concentration 32.43 mg/L, the maximum PEN G was 95% (9.14 mg/g). The Freundlich and Langmuir isotherms and pseudo-second-order models gave the best-fit to equilibrium experimental adsorption data. The findings of the study showed that new modified magnetic nanoparticles-graphene using ionic liquid (ILMNPs) can use as a high potential, simple, rapid separation, and re-generable material for adsorption pharmaceuticals.

Keywords: Adsorption; Magnetic nanoparticles; Graphene oxide; Ibuprofen; Penicillin G

1. Introduction

Penicillin G or benzyl penicillin (R:benzyl) is mostly used in the modern industrial livestock operations and human medicine. Penicillin G is water-soluble (210 mg/L) and has a biological half-life of 30–60 min and is primarily excreted through the kidneys. In recent years, reports of PEN G in raw sewage and treated effluent have measured 153 and 1.68 mg/L, respectively [1]. Ibuprofen ($C_{13}H_{18}O_2$) belongs to a group of drugs called non-steroidal anti-inflammatory drugs (NSAIDs). It is also one of the most widely consumed NSAIDs in the world. It presents in wastewater treatment plants (WWTPs) at concentrations of up to 3 μg/L and in rivers and lakes, detected at concentrations of up to 8 ng /L (soluble in water at 21 mg/L) [2]. The United States Environmental Protection Agency's acceptable level for pharmaceuticals in effluent is 1 μg/L [3]. Pharmaceuticals and personal care products (PPCPs) removal technologies

* Corresponding author.
† Co-first author.

from aquatic environment mainly include biological processes, adsorption, photolysis, chemical-, and advanced-oxidation methods [4]. The conventional treatment processes in WWTPs are not usually effective in removing or degrading the majority of these compounds. The PPCPs can be partially eliminated in biological treatment systems; therefore, residual quantities remain in treated water and can accumulate in drinking (tap) water [5]. Such biological treatment systems as activated sludge and biological trickling filters are not able to eliminate the whole range of emerging pollutants and leaving more chemical compounds in water [6]. Although antibiotics' molecules degrade and decompose into simple compounds or are mineralized by chemical processes, especially advanced oxidation processes, these processes are very expensive and hard to operate [7]. Absorption is a versatile treatment technique practiced widely for the removal of dissolved organics from water and various adsorbents have been examined for organic contaminants so far [8,9]. Also, it is a promising way to remove various organic compounds because of its interesting properties encompass simple design and easy to operate, high efficiency, low cost, etc. [10–13]. However, there is still an increasing demand for the advancement of efficient and affordable treatment technologies for the elimination of water-borne pollutants. Carbon-based materials have been successfully used as solid adsorbents in solid-phase extraction (SPE) due to their large specific surface area and excellent adsorption capacity. Graphene oxide (GO) has unique physical and chemical characteristics and has become a major research target, but the GO-based adsorbents are limited due to hard to separation and centrifugation, and increase the required pressure in filtration [21]. The separation methods are underground at a high cost, additional operation units, and also are time-consuming [4]. Therefore, separation technology based on magnetic adsorbents has been recently suggested to respond to these limitations. This way accompanies for an easy filtration or centrifuge by an external magnetic field that achieves solid–liquid [14]. Recently, magnetic separation technique has attracted a lot of literatures based on magnetic iron oxide nanoparticles (MNPs) [15]. It has potential applications in many studies fields such as chemistry, medical, genetics, etc. Ionic liquids (ILs) are in the class of organic salts which are composed of organic cations and inorganic or organic anions [16]. The ILs possesses many unique physicochemical properties, such as good stability, low toxicity, negligible vapor pressure, and tuneable miscibility [17]. Thus, they are regarded as promising "green" materials for a number of analytical applications [16]. This study aimed to evaluate the adsorption potential of a new modified magnetic nanoparticles-graphene using ionic liquid (ILMNPs) method to adsorb of two pharmaceuticals (ibuprofen and penicillin G) from synthetic solutions. Therefore, analyzing, optimizing, and identifying the interaction between variables response surface methodology (RSM) were employed. Based on the available database, similar works have not been reported.

2. Experimental

2.1. Materials

A modified magnetic nanoparticles-graphene hybrid was prepared in the laboratory of Tehran Pharmaceutical University. Penicillin G and ibuprofen were purchased from Farabi Pharmaceutical Company is located in Isfahan, Iran. Other chemicals used were purchased from Germany's Merck. The contaminated water used in the experiments was prepared from mixing aliquots of PEN G and IBU stock solutions (1,000 mg/L) with distilled water.

2.2. Synthesis of graphene oxide

The GO was synthesized from the graphite powder according to the modified Hummer method [17]. Briefly, 2 g of graphite powder and 2 g of $NaNO_3$ were added to 92 mL H_2SO_4 (98%) in a flask and stirred in an ice bath, and then 2 g of $KMnO_4$ were added to the above solution. After stirring for 0.5 h, the ice bath was removed and this mixture was stirred at 35°C for 6 h. Afterward, the mixture was diluted with 160 mL of the DI water. Then, the resulting mixture was stirred at 90°C for 2 h. After that 400 mL of DI water was added and followed by the addition of 12 mL of H_2O_2 (30 %) to end the reaction, upon which the color of the mixture turned to a bright yellow. For purification, the obtained mixture was washed with a 1:10 HCl solution (150 mL) and DI water many times to remove metal ions. The obtained dispersion was sonicated at 130 KHz for 2 h and centrifuged to remove any un-exfoliated GO [18,19].

2.3. Synthesis ionic liquid modified magnetic nanoparticles-graphene hybrid (Fe_3O_4@GO-IL)

The preparation of GO–Fe_3O_4 occurred through the co-precipitation of Fe^{3+} and Fe^{2+} in the presence of GO. Schematics of the chemical path to the synthesis and structure of Fe_3O_4@GO-IL functionalized is illustrated in Fig. 1. To prepare nanoscale magnetite, a molar ratio of Fe(II)/Fe(III): 0.5 is essential. For the GO–Fe_3O_4 synthesising, 40 mg of GO was dispersed in 40 mL of deionized water using an ultrasonic water bath for 30 min. Then 600 mg $FeCl_3{\cdot}6H_2O$ and 300 mg $FeCl_2{\cdot}4H_2O$ were dissolved in 50 mL of deionized and degassed (with ultrasonic) water and added to the previous solution. Then the mixture was heated to 85°C. This solution mixture was dropped into a beaker containing NH_3 solution (30%) under nitrogen gas and it was stirred vigorously for 45 min to prevent the oxidation of Fe^{2+} ions. The mixture was heated to 85°C [20]. The system was then cooled to room temperature. In the next step, the mixture was separated by an external magnetic field. The resultant black product was rinsed with water and then dried at 60°C under nitrogen atmosphere. For synthesizing Fe_3O_4@GO-IL, 3 mL of ionic liquid-based organosilane functionalized by imidazole (I) was dispersed in a mixture of 200 mg Fe_3O_4@GO and 250 mL toluene and then was refluxed for 24 h. The solid product was collected and washed with DI water and ethanol by magnetic separation and then vacuum dried.

2.4. Batch adsorption studies

For each adsorption test, different volumes containing known quantities of as-dispersed Fe_3O_4@GO-IL were added to 10 mL solution having predominated concentrations of the IBU and PEN G. The pH level of the solution was adjusted to the desired value by using HCL and

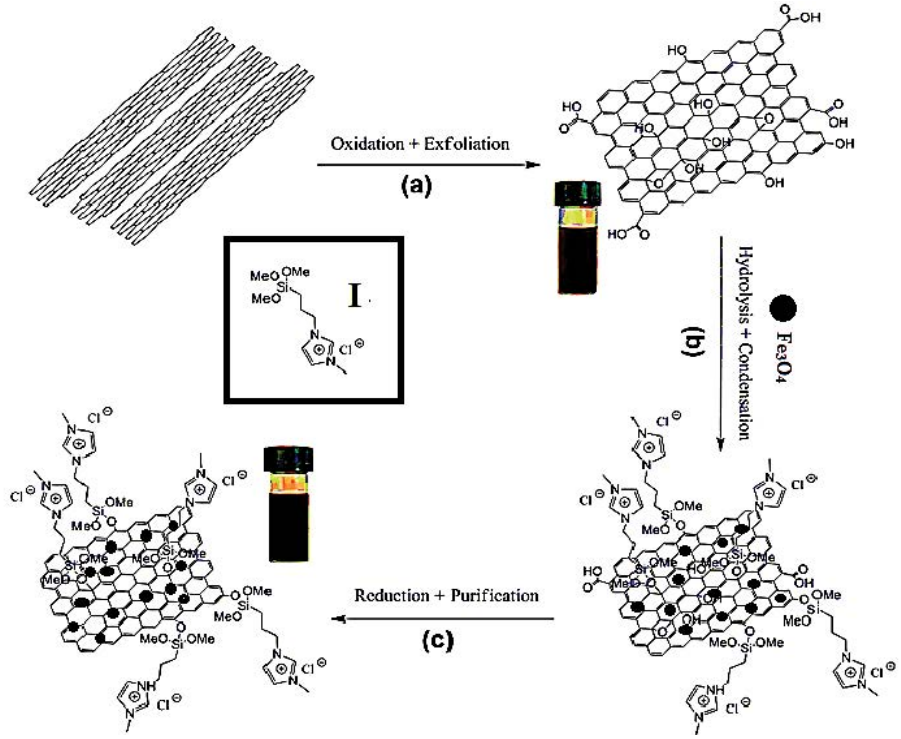

Fig. 1. (a–c) Schematics of the chemical path to the synthesis and structure of Fe_3O_4@GO-IL functionalized.

NaOH (0.1 mol/L). All solutions underwent constant mixing at 950 rpm for different contact times determined by the experimental design. After the adsorption process, the nano-adsorbent was eliminated rapidly from the aqueous solutions using a magnet. The wavelengths of maximum adsorption of IBU and PEN G are 223 [21] and 215 nm, respectively, which are determined by a UV-vis spectrophotometer. Stock solutions of PEN G and IBU (1,000 mg/L) were produced by dissolving 1 g of analytical grade PEN G and IBU in distilled water. The removal percentage (R%) of PPCPs on nanoparticles was calculated using Eq. (1). Also Eq. (2) was used to obtain the maximum adsorption capacity.

$$R(\%) = \frac{\left(\mathrm{PPCPs}_0 - \mathrm{PPCPs}_e\right) \times 100}{\mathrm{PPCPs}_0} \tag{1}$$

$$q_e = \left[\frac{\mathrm{PPCPs}_0 - \mathrm{PPCPs}_e}{m}\right] \times v \tag{2}$$

where the PPCPs_0 is the initial PPCPs concentration (mg/L), v is the volume of the solution (L), the PPCPs_e is the equilibrium PPCPs concentration in solution (mg/L), and m is the weight of nanoparticle (g).

2.5. Experimental design

RSM based on a CCD was used to optimize the removal of IBU and PEN G by adsorption onto Fe_3O_4@GO-IL. Central composite design (CCD) was used to investigate IBU and PEN G removal. The RSM was employed to evaluate the combined effects of pH, Fe_3O_4@GO-IL dose, contact time, and initial IBU and PEN G concentration on the adsorption process. These variables were investigated at five levels. In the present study, the Minitab software package was used to design and evaluate these five independent variables at five response levels. The details of 30 experiments are presented in Table 1.

3. Results and discussion

3.1. Characterization of Fe_3O_4@GO-IL

Fabricated Fe_3O_4@GO-IL was characterized with multiple techniques including scanning electron microscopy (SEM), transmission electron microscopy (TEM), and the FT-IR spectra, which are represented in Fig. 2. The three-dimensional images produce by SEM is revealed that the morphologies properties such as the shape of and the location of features in fabricated Fe_3O_4@GO-IL (Fig. 2a). With focusing on the nano-magnetic particles surfaces and its composition, it is obvious that a uniform distribution and consequently, a smooth surface were provided during the ionic liquid modification process. This fact can be attributed to the high viscosity of ionic liquid that infiltrated into the void space of graphene sheets. The TEM of nanoparticles was taken to get a two-dimensional cross-section, a more magnification, and a greater resolution of the Fe_3O_4@GO-IL. According to the TEM image (Fig. 2b), more details about internal composition as graphene sheet and Fe_3O_4 were seen. In order to detection of the vibration characteristics of chemical functional groups in synthesis nano-magnetic particles FT-IR spectra were taken. However, to comparison between GO and Fe_3O_4@GO-IL, this test was conducted and the result of that is illustrated in Fig. 2c. It is evidence that

Table 1
Experimental plan based on CCD and the results

Entry	Ibuprophen					Penicillin G				
	pH	Time (min)	Initial concentration (mg/L)	Adsorbent dose(g/L)	Removal efficiency	pH	Time (min)	Initial concentration (mg/L)	Adsorbent dose(g/L)	Removal efficiency
1	6	65.0	12.50	0. 125	98.71	6	75.0	27.50	0.3	72.62
2	4	37.5	8.75	0.087	87.39	6	75.0	5.00	0.3	24.54
3	6	65.0	12.50	0.125	98.16	4	52.5	16.25	0.2	67.00
4	6	65.0	12.50	0.050	89.25	8	97.5	16.25	0.2	35.35
5	8	92.5	8.75	0.087	47.94	6	75.0	27.50	0.3	71.31
6	6	65.0	20.00	0.125	90.54	8	52.5	16.25	0.4	8.73
7	4	37.5	8.75	0.162	73.72	4	97.5	16.25	0.4	70.78
8	4	37.5	16.25	0.162	56.82	2	75.0	27.50	0.3	87.72
9	6	65.0	12.50	0.125	98.34	8	97.5	16.25	0.4	18.43
10	8	92.5	8.75	0.162	50.39	6	75.0	50.00	0.3	71.97
11	8	37.5	16.25	0.087	63.16	8	97.5	38.75	0.4	49.25
12	6	65.0	12.50	0.200	91.85	4	52.5	16.25	0.4	62.56
13	4	92.5	8.75	0.087	84.68	6	75.0	27.50	0.3	72.36
14	4	37.5	16.25	0.087	89.34	8	52.5	16.25	0.2	50.27
15	4	92.5	16.25	0.162	79.79	6	120.0	27.50	0.3	77.22
16	8	92.5	16.25	0.162	82.62	4	97.5	38.75	0.2	94.39
17	8	37.5	8.75	0.087	38.75	6	75.0	27.50	0.3	71.84
18	10	65.0	12.50	0.125	44.04	10	75.0	27.50	0.3	58.16
19	8	37.5	16.25	0.162	63.16	4	52.5	38.75	0.4	42.23
20	6	65.0	12.50	0.125	98.53	8	52.5	38.75	0.2	63.57
21	6	120.0	12.50	0.125	92.96	4	52.5	38.75	0.2	80.67
22	6	65.0	12.50	0.125	97.97	4	97.5	16.25	0.2	79.61
23	8	92.5	16.25	0.087	59.43	6	75.0	27.50	0.1	61.86
24	8	37.5	8.75	0.162	45.18	2	75.0	27.50	0.3	88.90
25	6	65.0	5.00	0.125	81.94	8	52.5	38.75	0.4	48.72
26	4	92.5	16.25	0.087	71.83	8	97.5	38.75	0.2	53.61
27	6	10.0	12.50	0.125	88.13	6	75.0	27.50	0.3	71.57
28	2	65.0	12.50	0.125	54.94	4	97.5	38.75	0.4	90.03
29	6	65.0	12.50	0.125	98.01	6	30.0	27.50	0.3	72.36
30	4	92.5	8.75	0.162	74.88	6	75.0	27.50	0.5	80.50

the new changes at the 2,897; 1,725; 1,630; 1,365; 1,246; and 572 cm^{-1} areas have been created. These changes are related to the characteristic of the C–H stretching, C=O, C–H, C–O, and Fe–O groups, respectively.

3.2. ANOVA and regression model

Four effective parameters including initial pH, contact time, PPCPs concentration levels, and Fe_3O_4@GO-ILs dosage were considered for designing the experiment conditions. The ranges of these variables for each PPCP are presented in Table 1. The results from all 30 experimental runs are displayed in Table 2. To verify the fitting of model, statistical constants, and values such as correlation coefficient (R^2), and adjusted R^2 between the experimental and predicted model values were calculated. The R^2 values for IBU were 0.86 and 0.72, and 0.82 and 0.62 for PEN G, respectively. The statistically significant index, *P*-values, for IBU and PEN G adsorption models were determined about <0.01 and <0.01, respectively. These results are shown that the models to be highly significant, with a probability of $P < 0.05$. The adequate precision is measure of the experimental signal-to-noise ratio which supports proper validity of the analysis. An adequate precision greater than 4 (IBU = 9.87 and PEN G = 11.2) implies validity and reliability of analysis. Regarding these amounts are provided appropriate criteria for validation. The absorption models were calculated from the actual factors as Eqs. (3) and (4). The final equation in terms of actual factors:

$$\text{IBU removal (\%)} = 20.022 + (17.900 \times \text{pH}) + (0.281 \times \text{contact time}) + (4.398 \times \text{IBU concentration}) - (-161.301 \times \text{nanoparticle dose}) + (0.904 \times \text{pH} \times \text{IBU concentration}) + (79.889 \times \text{pH} \times \text{nanoparticle dose}) + (3.930 \times \text{time} \times \text{nanoparticle dose}) + (-3.545 \times \text{pH}^2) - (0.005 \times \text{time}^2) - (0.363 \times \text{IBU concentration}^2) \quad (3)$$

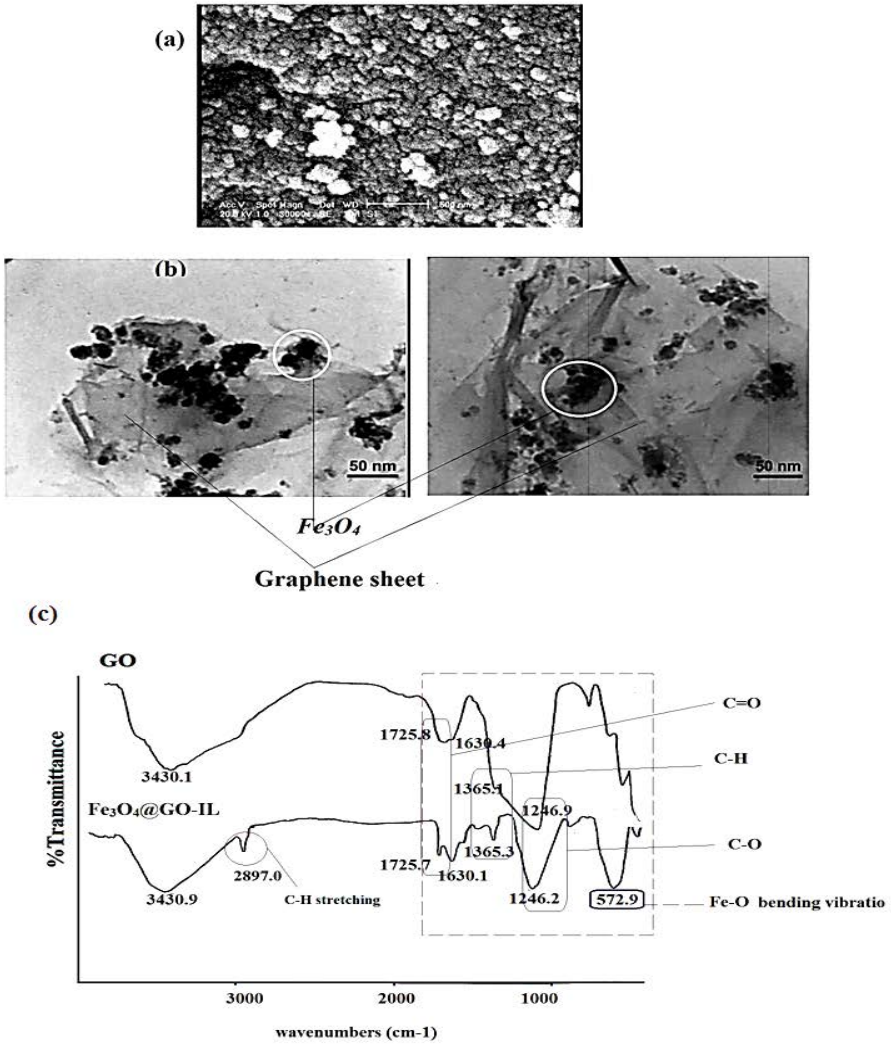

Fig. 2. SEM (a), TEM (b), FT-IR spectra, and (c) of Fe_3O_4@GO-IL.

Table 2
The variables studied in the evaluation of the ability of magnetic nanoparticles as nano-adsorbents (α = 2)

Variables($\pm\alpha$) PPCP	pH	Contact time (minute)	PPCP concentration (mg/L)	Fe_3O_4@GO-IL dosage (g/L)
IBU	2–10	10–120	5–20	0.05–0.20
PEN G	2–10	30–120	5–20	0.10–0.50

PEN G removal (%) = +94.865 – (2.248 × pH) + (0.404 × contact time) – (0.420 × PEN G concentration) – (175.211 × nanoparticle dose) – (0.133 × pH × time) + (0.197 × pH × PEN G concentration) + (1.810 ×time × nanoparticle dose) (4)

3.3. Optimization condition and conformity

The main goal of the optimization process was to determine optimum values for variables influencing the removal of IUB and PEN G by Fe_3O_4@GO-IL. The theoretical results indicated that maximum adsorption of IUB 100% by Fe_3O_4@GO-IL could be achieved at a pH of 5.6, initial concentration of 12 mg/L, time of 72 min, and sorbent dosage of 0.14 g/L. Similarly, optimum conditions for PEN G were determined such as pH 4, initial concentration of 32.5 mg/L, contact time of 97.5 min, and sorbent dosage of 0.3 g/L. The validity of the optimized values given by the model was confirmed by two experiments for both of IUB and PEN G were carried out. These points were shown in Figs. 2a and b. Experimentally, the maximum removals for

IUB and PEN G were 97.58 (~5 mg/g) and 95% (24.5 mg/g), respectively. These results verified that the experimental values are in good agreement with the predicted values according to confidence interval (CI) 95%. This fact can corroborate the model which is successful in predicting the responses.

3.4. Parametric study

The effects of varying experimental parameters to the sorption of IBU are depicted in Fig. 3. Referring to these plots, it can be found that the IUB adsorption efficiency is reached to more than 97.58 (~5 mg/g). Generally, an increase in adsorbent dose, IUB, and contact time caused an improvement in total IUB adsorption efficiency and uptake. These facts are shown in Figs. 3a–c. Adsorbent dosage of the magnetic nanoparticles was considered due to the effect on IUB adsorption efficiency from the solution. Husein [22] showed that when the adsorbent dose was small, the binding sites on the adsorbent surface were also small so the adsorption efficiency was low. The contact time as other important variables was considered for the interactions between IUB and nano-magnetic particles. Increasing sorption efficiency with an increase in contact time is related to enough time to occupy the active site by the IUB molecules. The adsorption uptake of IUB decreased with a higher amount of nano-magnetic particles due to an increase in the surface area containing sorption sites regard to a constant IBU concentration. Lower adsorption percentage with lower concentration of IUB is probably due to the limitation of the mass transfer of IUB molecules from the bulk solution to the boundary layer and active sites. Banerjee et al. [23] also represented an increase in IBU concentration in the solution that can be caused by an accumulation of IBU molecules around the active sites of adsorbent, resulting in higher percentage removal of IBP. Contrary to this fact, a further rise in IBP concentration can lead to a decrease in IBP removal percentage because it may occurred due to the exhaustion of all available active sites by adjacent IBP moieties [4]. Rafti et al. [24] showed that the IBU removal is increased by increasing the initial concentration. This fact is due to a considerable driving force for overcoming all mass transfer resistance between aqueous and solid phases [25]. The adsorption efficiency rapidly decreased with increasing solution pH. These variations were more impressive on removal percentages (Fig. 3c). The pH plays an imperative role in separation science due to the effect of the ionization degree of adsorbed matters and the dissociation of surface functional groups [26].

Pharmaceuticals like IUB and PEN G exist in the neutral form at pH below pK_a (pK_a is the negative base-10 logarithm of the acid dissociation constant of a solution), and also, those are in anionic form when the pH is above pK_a. The pK_a for IUB is about 4.52 and it can facilitate ionize at acidic pH, especially below than 4.52. According to the results, higher adsorption is observed in acidic medium. It was mainly ascribed to the electrostatic interaction and inclusion complexes between the adsorbate and IBU. There are some similar results in agreement with this fact [27,28].

As PEN G data, the adsorption efficiency were determined in ranges of 8.73 (0.17 mg/g) to 94.4% (9.14 mg/g). Generally, graphene based adsorbents are strongly dependent on pH of the solution. The pH point of zero charges (or pH_{pzc}) of graphene/graphene oxide-based material are about 3.9 and 6.1, and these amounts are related to the positive and negative charges on adsorbent in acidic and basic solutions, respectively. As seen in Fig. 4, there are the effects of various parameters on PEN G removal efficiency during the adsorption process. Similar to IBU, overall adsorption progress improved by increasing the adsorbent dose, contact time, and initial PEN G concentration up to 0.4 g, 97.5 min, and 38.75 mg/L, respectively. Under this condition, removal efficiency of about 94.4% was achieved. Rahdar et al. [29] reported the removal efficiency of PEN G onto magnesium oxide nanoparticles increased speedily with an increase in the adsorbent dose from 0.3 to 1.5 g/L. Maximum removal of PEN G was observed at an adsorbent concentration of 1.5 g/L (q_m = 2 mg/g, R = 70%). This was

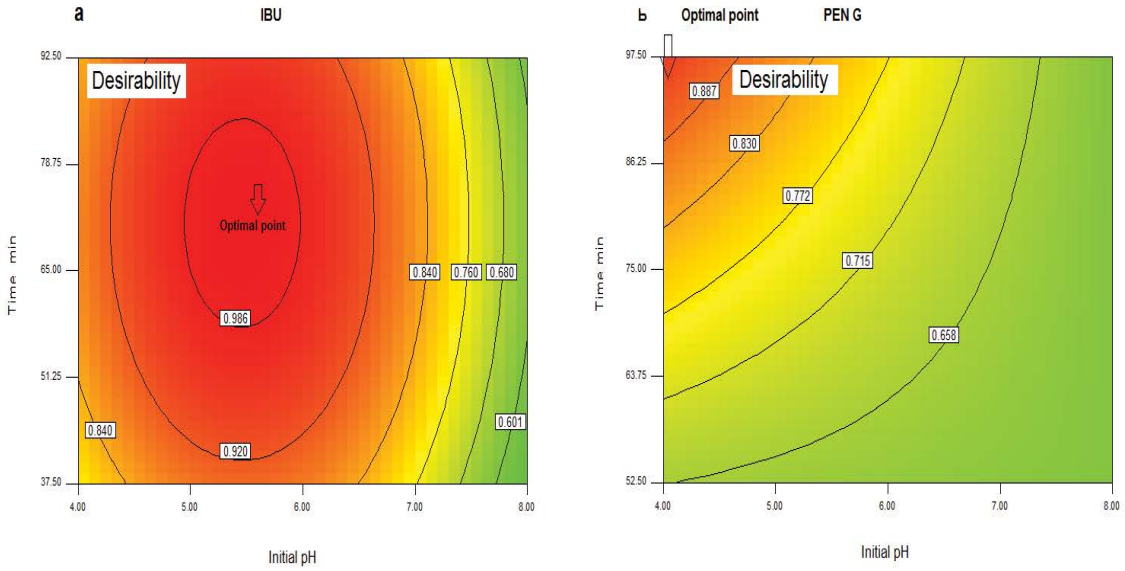

Fig. 3. Optimal condition for adsorption of IBU (a) and PEN G (b).

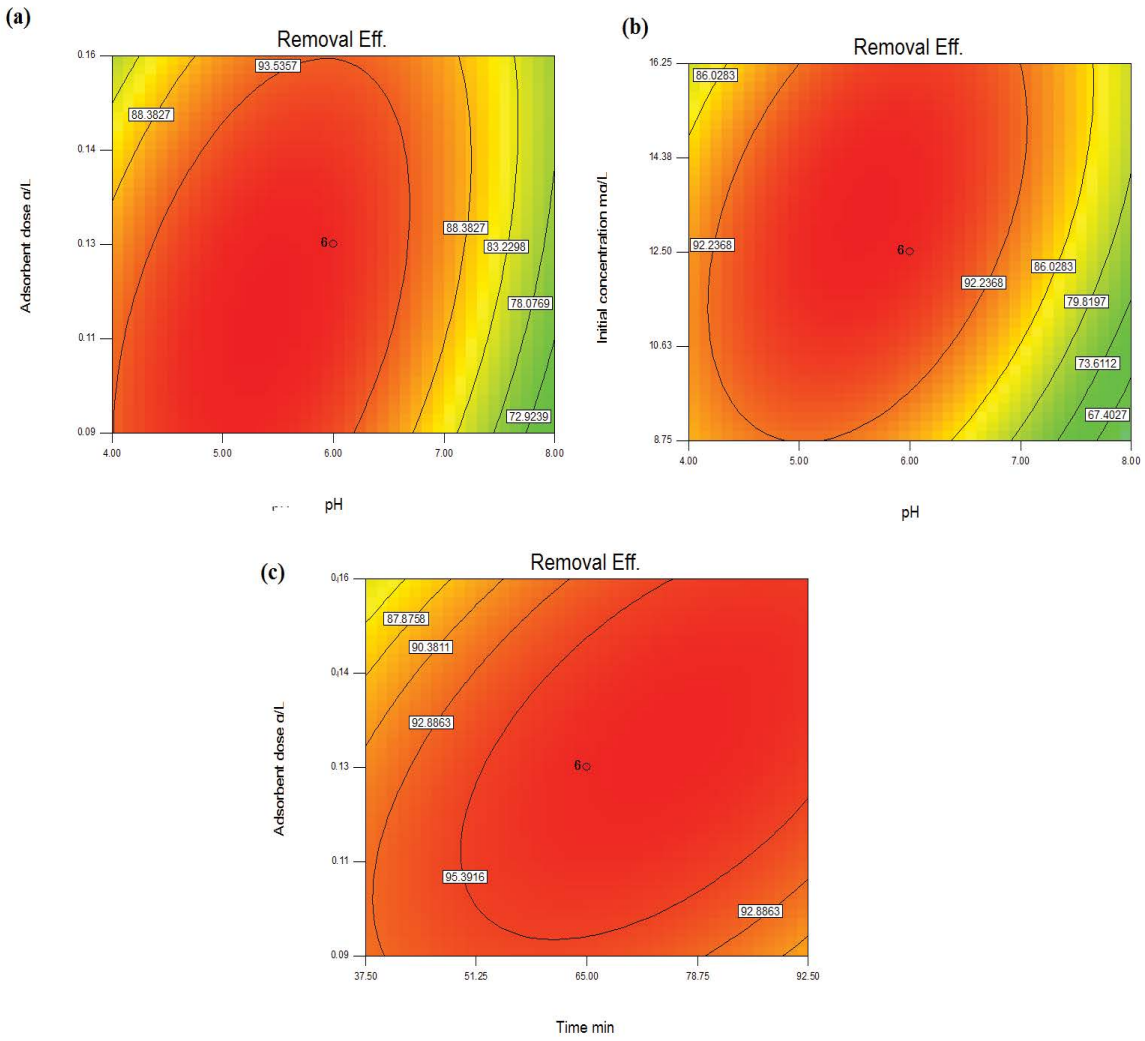

Fig. 4. (a–c) Effects of various parameters on IBU removal efficiency.

because of an increase in the number of available adsorption active sites that results in an increase in adsorption capacity [30]. Moreover, the adsorption efficiency rapidly decreased with pH greater than 4. Thus, acidic conditions were more optimal for the removal of PEN G. PEN G is a weak monocarboxylic acid with a pK_a about 2.75 which that easily is dissociated at pHs more than pK_a, as a result at higher pH values, the ionization degree of PEN G increase. In this situation, the electrostatic repulsion between the negatively charged surface sites and PEN G ions increases. Consequently, adsorption percentage of PEN G is declined. Similar results were reported by Balarak et al. [31] and Alnajrani et al. [32]. Rahdar et al. [29] showed that the maximum removal rate of PEN G onto magnesium oxide nanoparticles was obtained at pH 3. Shammala and Chiswell [10] reported similar results, an acidic environment is more favourable to enhance the degradation of pharmaceutical on graphene based nanocomposite derivatives with magnetic chitosan nanocomposite. The pH value affects the protonation of the available surface groups (change the adsorbent charge), and consequently affect on the chemical form of adsorbate in the bulk solution, so that with increasing pH, the adsorption rate will decrease. Nguyen et al. [33] showed that the removal rate of IBU in acidic pH of solutions.

To compare the potential of magnetic nanoparticle for pharmaceutical compound literatures were viewed. As shown in Table 3, the adsorption of some pharmaceuticals by various adsorbents is represented. Referring to this studies and their uptake (and also adsorption efficiency), it can be concluded that the magnetic nanoparticles are high potential adsorbents to remove the pharmaceutical like IUB and PEN G.

3.5. Reusability of Fe_3O_4@GO-IL

The interest in the reusability of adsorbents such as nanosorbents and new material is growing regarding economic and environmental aspects. Therefore, the regeneration ability of the adsorbent is an important factor influencing its practical application. The main advantage of nano-adsorbent [Fe_3O_4@GO-IL] is that it can be easily recycled, compared to most other adsorbents. The process of Fe_3O_4@GO-IL adsorbent recovery is much faster and easier than for previous species such as zeolite. In

Table 3
Literature review for adsorption of IUB and PEN G by various adsorbents

Pharmaceutical	Adsorbent	Kinetic	Isotherm	Uptake (mg/g) and adsorption efficiency (%)	References
IUB	Functionalized strong nano-clay composite	Elovich model	–	1.1 mg/g (94.3%) pH = 6	[24]
	Polymeric resin	Pseudo-second-order	Langmuir–Freundlich	18 mg/g	[43]
	Metal-organic framework MIL-53(Fe)	–	Langmuir	80.8%	[33]
	Ethylenediamine-GO	Pseudo-first-order	Freundlich	–	[44]
	GNP	Pseudo-second-order	Langmuir	3.72 mg/g	[44]
	Fe_3O_4@GO-IL nano-adsorbent	Pseudo-second-order	Langmuir	1.300–9.700 mg/g (45%–89.3%)	Present work
PEN G	*Lemna minor*	Pseudo-second-order	Langmuir	94.6% (36.18 mg/g)	[31]
	Modified canola	Pseudo-second-order	Langmuir	11.1 mg/g	[45]
	Polymer of intrinsic microporosity	Pseudo-second-order	Freundlich	80%	[32]
	Fe_3O_4@GO-IL nano-adsorbent	Pseudo-second-order	Freundlich	0.170–9.140 mg/g (8.73%–94.4%)	Present work

order to evaluate the possibility of regeneration and reuse of the Fe_3O_4@GO-IL nano-adsorbent, particles were stirred in hot hydrochloric acid 1 M (HCl) for 12 h to remove contaminants. Then the adsorbent was washed with ethanol several times and collected magnetically from the solution. After elution, the adsorbent was dried in a vacuum oven at room temperature for 24 h and reuse. Fig. 6 represents the reusability results of Fe_3O_4@GO-IL nano-adsorbent for the adsorption of IUB and PEN G. To evaluate the reusability potential of the Fe_3O_4@GO-IL, four times recycling were considered. The adsorption efficiency of IUB decreased from ~98% to ~84%, during four repeated cycles. In the same away, inconsiderable decrease in removal percentage from 95% to 86% was seen for PEN G. The findings were demonstrated that the nano-adsorbent to be reusable with negligible loss in its sorption behavior.

3.6. Kinetic and equilibrium studies

Kinetic and isotherm analyses were performed using the most popular related models and equations; in particular, Langmuir and Freundlich isotherms, pseudo-first-order, and pseudo-second-order kinetic models. Adsorption kinetic and isotherm of IUB and PEN G were evaluated at optimal conditions.

The Langmuir isotherm is expressed as the following equation [34]:

$$\frac{1}{q_e}=\left(\frac{1}{q_{\max}K_L}\right)\left(\frac{1}{C_e}\right)+\left(\frac{1}{q_{\max}}\right) \tag{5}$$

where q_e is the amount of PPCPs adsorbed at equilibrium (mg/g), C_e is the equilibrium PPCPs concentration in water samples (mg/L), K_L is the Langmuir constants of adsorption (L/mg), and $q_{\max}$ is the maximum adsorption capability (mg/g).

The Freundlich model is expressed as the following equation [35]:

$$\log q_e=\log K_f+\frac{1}{n}\log C_e \tag{6}$$

where K_F is the constant related to overall adsorption capacity (mg/g(mg L)$^{-1/n}$)

$1/n$ is the constant related to surface heterogeneity (dimensionless).

The isotherms values and constants for two PPCPs are observed in Table 4. Accordingly, it is evident that the experimental data for IBU and PEN G is fitted to Langmuir (R^2 = 0.982) and Freundlich (R^2 = 0.996) models, respectively. The Langmuir isotherm is indicated monolayer coverage of IUB on nanoparticles. The results of this study are in agreement with prior reports of adsorption for PEN G and IUB (Table 4). Also, a remarkable amount of $q_{\max}$ for IBU (25.504 mg/g) and PEN G (21.012 mg/g) is suggested by the models. Banerjee et al. [23] reported that adsorption of ibuprofen from aqueous by graphene oxide nanoplatelets fitted the Langmuir isotherm. Also, Masoudi et al. [36] showed that the adsorption of Penicillin G by silica nanoparticles was more consistent with Langmuir model (R^2 = 0.810). Bhadra et al. [37] confirmed that adsorptive removal of IBU from water using metal-organic framework-derived porous carbon is in a good agreement with Langmuir isotherm.

Adsorption kinetic parameters of studied PPCPs onto nanoparticles were modeled by five kinetic models, pseudo-first-order, pseudo-second-order, and diffusion models (intraparticle, Bangham, and Boyd). Adsorption kinetics

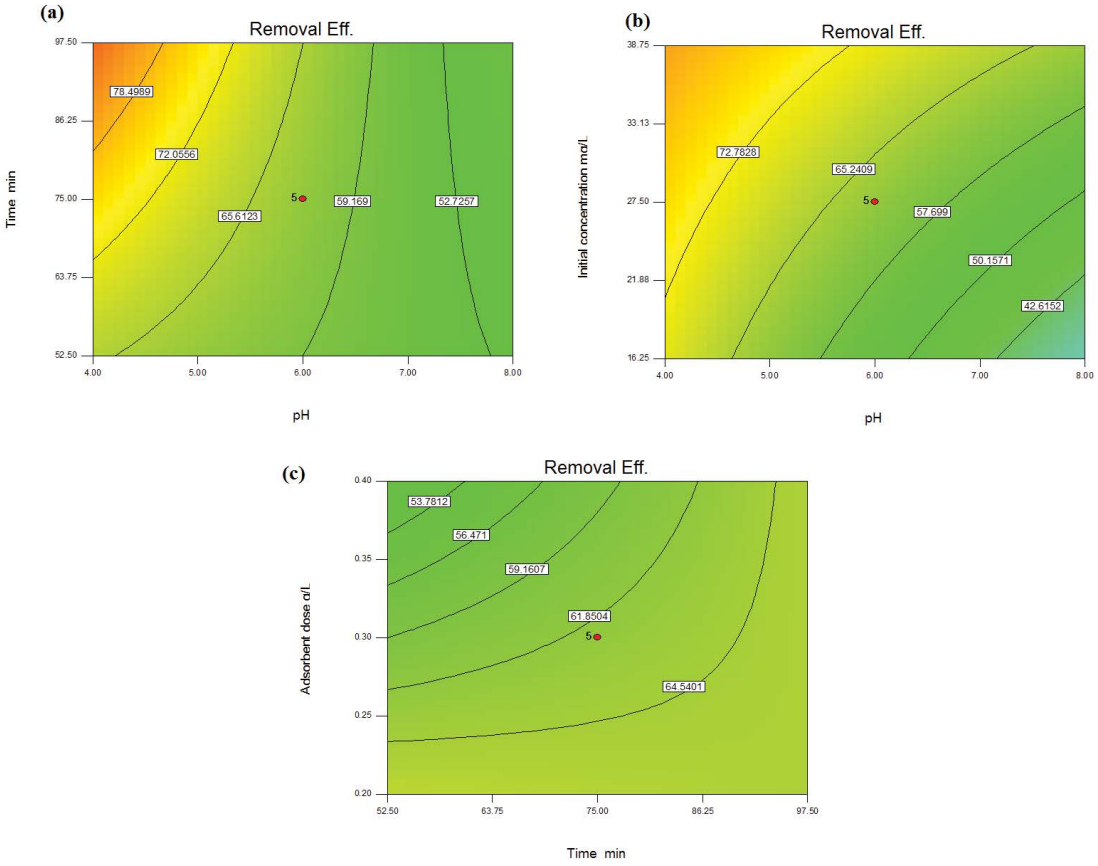

Fig. 5. (a–c) Effects of various parameters on PEN G removal efficiency.

Table 4
Langmuir and Freundlich isotherm parameters for penicillin G and IUB adsorption

	Langmuir model			Freundlich model		
Adsorbate	q_{max}	K_L (L/mg)	R^2	K_F (mg$^{n-1/n}$/g/L)	n_f	R^2
IBU	21.012	0.014	0.982	1.352	1.232	0.955
PEN G	24.504	0.004	0.981	0.233	0.963	0.996

must be investigated in order to determine the time necessary for reaching equilibrium and to elucidate the mechanism of the adsorption process. The pseudo-first-order equation, also known as Lagergren equation can be expressed as follows in Eq. (7):

$$\log\left(q_e - q_t\right) = \log q_e - k_1 t \tag{7}$$

Here k_1 is the adsorption rate constant (S^{-1}), q_t is the amount of solute adsorbed at time t (mg/g), and q_e is the amount of solute adsorbed at saturation (mg/g).

While pseudo-second-order kinetic equation can be expressed as follows [38]:

$$\frac{t}{q_t} = \left(\frac{1}{k_2 q_e^2}\right) + \frac{t}{q_e} \tag{8}$$

where k_2 is the adsorption rate constant of pseudo-second-order model.

As seen as in Eqs. (9)–(11), there are the equations of three most popular diffusion models consisting; intraparticle, Bangham, and Boyd, respectively [39].

$$\log q_t = \log k_{id} + \alpha \log\left(t\right) \tag{9}$$

$$\log\left[\frac{C_0}{C_0 - q_t m}\right] = \log\left[\frac{k_0 m}{2.303V}\right] + \alpha \log t \tag{10}$$

$$B_t = -0.4977 - \ln\left(1 - F\right) \tag{11}$$

where k_{id} is the adsorption rate and constant of intraparticle model, V the volume of solution (L), m the mass of

adsorbent (g), k is the adsorption constants, B is a constant, and F is the fractional attainment of equilibrium (q_t/q_e).

Comparing the correlation coefficients and kinetic constants deviated from sorption data, the models suggest that the sorption of IUB and PEN G onto the ionic liquid modified magnetic nanoparticles-graphene has good conformity with the pseudo-first and second-order ($R^2 = 0.998$) and Boyd models (Tables 5 and 6). At among the diffusion kinetics, the Boyd had higher fitting by its R^2. Also, all diffusion models were more coincidence with PEN G adsorption data. Higher coloration with second-order kinetic implies that the sorption rate depends on second power of PPCPs concentrations. Better fitting by R^2 rather than first-order model indicates the adsorption behavior involved valence forces by sharing of electrons between IBU, PEN G, and magnetic adsorbent. Similarly, Chen et al. [28] showed that adsorption kinetics of IBU on ferroferric oxide nanoparticles (doubly coated with chitosan and β-cyclodextrin) was fitted with pseudo-second-order kinetic [28], also, for PEN G by [40]. Chavoshan et al. [41] displayed adsorption of PEN G from aqueous solutions by single-walled carbon nanotubes (SWCNTs) has the highest correlation with pseudo-second-order model.

3.7. Error analysis

It has been found that the error structure is a key to judge about experimental data when the transformation of adsorption isotherms into their linearized forms is occurred [42]. Although, in determine the error analysis, many formulas like; the sum square of errors (ERRSQ), the hybrid fractional error function (HYBRID), average relative error (ARE), and others are popular, but the coefficient of non-determination (CN) is a simple method. Also, CN is very valuable tool for describing the extent of the relationship between the transformed experimental data and the predicted isotherms and minimization of the error distribution. CN can be calculated from Eq. (12) [42]:

$$CN = 1 - R^2 \tag{12}$$

The CN for kinetic and isotherm models used in this study are represented in Table 7. According to CNs, it is clear that the better fit was for second-order kinetic.

Table 6
Adsorption kinetic parameters of studied PPCPs onto nanoparticles modeled by diffusion kinetic models, intraparticle, pseudo-second-order

Kinetics	Intraparticle		Bangham		Boyd	
Adsorbate	k_{id}	R^2	α	R^2	B	R^2
IBU	0.181	0.454	0.060	0.544	0.086	0.891
PEN G	0.642	0.970	0.020	0.970	0.031	0.779

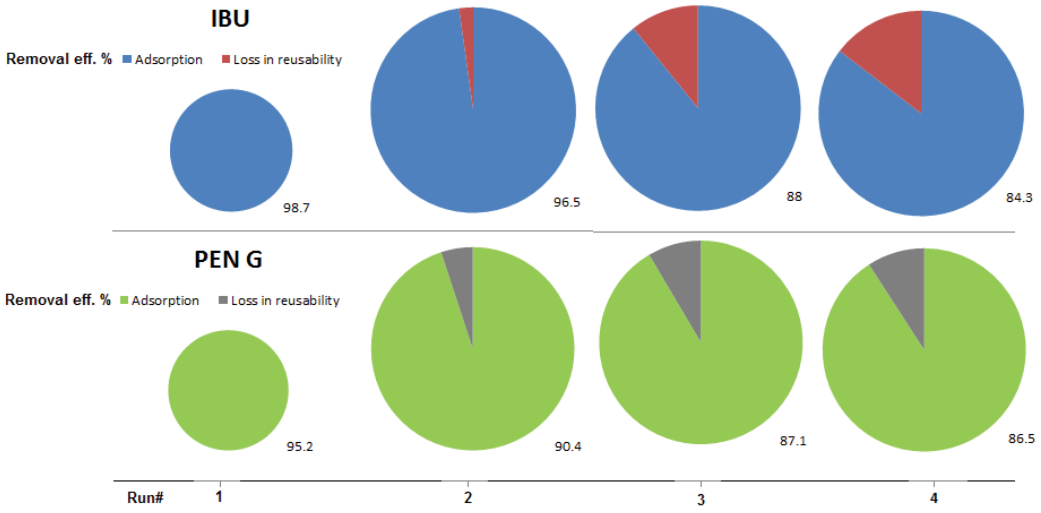

Fig. 6. Reusability potential of the magnetic nanoparticle.

Table 5
Adsorption kinetic parameters of studied PPCPs onto nanoparticles modeled by two kinetic models, pseudo-first-order, and pseudo-second-order

Kinetics	Pseudo-first-order			Pseudo-second-order		
Adsorbate	k_1 (1/min)	q_e	R^2	k_2 (g/mg min)	q_e	R^2
IBU	0.030	6.240	0.833	0.006	13.503	0.998
PEN G	0.012	2.889	0.921	0.012	10.401	0.998

Table 7
Coefficient of non-determination of kinetic and isotherm models

Kinetics	First-order	Second-order	Intraparticle	Bangham	Boyd
IBU	0.170	0.011	0.550	0.463	0.110
PEN G	0.080	0.011	0.030	0.032	0.219
isotherms	Langmuir	Freundlich			
IBU	0.020	0.050			
PEN G	0.020	0.010			

Also, the CNs of isotherm models, it seems that both of them have a high correlation with sorption data. The uptake and removal efficiencies were increased with increasing initial concentration of IBU and PEN G with regard to the literature review (Table 3). It can be observed that the most fitted kinetic model for IBU and PEN G were reported with pseudo-second-order kinetic.

4. Conclusion

According to the results of FTIR, SEM, and TEM, the Fe_3O_4@GO-IL was successfully prepared. These nanoparticles showed that formed superparamagnetic and could separate by a magnet after the adsorption process. The Fe_3O_4@GO-IL was represented that can use as a promising candidate for replacing conventional adsorbents in removing PPCPs. The maximum removals of both pharmaceutical (IBU and PEN G) from aqueous solution were higher than 95%. According to the data, Fe_3O_4@GO-IL possessed not only high adsorption capacity but also have good reproducibility. The Fe_3O_4@GO-IL was a high adsorption capacity even after four cycles of adsorption, indicating that it has an excellent regeneration performance. The adsorption kinetics and isotherms were also investigated in detail and confirmed the existence of high correlations between models and experimental data. Finally, results from reusability experiments revealed that it can be a stable and reusable adsorbent for PPCPs removal.

Ethical consideration

Ethical issues (including plagiarism, informed consent, misconduct, data fabrication and/or falsification, double publication and/or submission, redundancy, etc.) have been completely observed by the authors.

References

[1] A. Sheikh Mohammadi, M. Sardar, The removal of penicillin G from aqueous solutions using chestnut shell modified with H_2SO_4: isotherm and kinetic study, Iran. J. Health Environ., 5 (2013) 497–509.
[2] H.R. Buser, T. Poiger, M.D. Müller, Occurrence and environmental behavior of the chiral pharmaceutical drug ibuprofen in surface waters and in wastewater, Environ. Sci. Technol., 33 (1999) 2529–2535.
[3] R.S. Valverde, M.D.G. García, M.M. Galera, H.C. Goicoechea, Determination of tetracyclines in surface water by partial least squares using multivariate calibration transfer to correct the effect of solid phase preconcentration in photochemically induced fluorescence signals, Anal. Chim. Acta, 562 (2006) 85–93.
[4] X. Hu, Y. Zhao, H. Wang, X. Tan, Y. Yang, Y. Liu, Efficient removal of tetracycline from aqueous media with a Fe_3O_4 nanoparticles@ graphene oxide nanosheets assembly, Int. J. Environ. Res. Public Health, 14 (2017) 1495, doi: 10.3390/ijerph14121495.
[5] M.D. Hernando, M. Mezcua, A.R. Fernández-Alba, D. Barceló, Environmental risk assessment of pharmaceutical residues in wastewater effluents, surface waters and sediments, Talanta, 69 (2006) 334–342.
[6] T. Urase, T. Kikuta, Separate estimation of adsorption and degradation of pharmaceutical substances and estrogens in the activated sludge process, Water Res., 39 (2005) 1289–1300.
[7] G. Moussavi, A. Alahabadi, K. Yaghmaeian, M. Eskandari, Preparation, characterization and adsorption potential of the NH_4Cl-induced activated carbon for the removal of amoxicillin antibiotic from water, Chem. Eng. J., 217 (2013) 119–128.
[8] A. Fakhri, S. Adami, Adsorption and thermodynamic study of cephalosporins antibiotics from aqueous solution onto MgO nanoparticles, J. Taiwan Inst. Chem. Eng., 45 (2014) 1001–1006.
[9] H.A.M. Salim, S.A.M. Salih, R.A. Rashid, Removal of acid alizarin black dye from aqueous solution by adsorption using zinc oxide, Int. Res. J. Pure Appl. Chem., 11 (2016) 1–8.
[10] F.A. Shammala, B. Chiswell, Removal of chrysoidine Y from water by graphene-based nanocomposite derivatives with magnetic chitosan nanocomposite, Int. J. Appl. Pharm. Sci. Res., 4 (2019) 17–33.
[11] N. Mirzaei, A.H. Mahvi, H. Hossini, Equilibrium and kinetics studies of direct blue 71 adsorption from aqueous solutions using modified zeolite, Adsorpt. Sci. Technol., 36 (2018) 80–94.
[12] H. Hossini, A. Rezaee, S.O. Rastegar, S. Hashemi, M. Safari, Equilibrium and kinetic studies of chromium adsorption from wastewater by functionalized multi-wall carbon nanotubes, React. Kinet. Mech. Catal., 112 (2014) 371–382.
[13] N.M.S. Mohammed, H.A.M. Salim, Adsorption of Cr(VI) ion from aqueous solutions by solid waste of potato peels, Sci. J. Univ. Zakho, 5 (2017) 254–258.
[14] S.N. Nabavi, S.M. Sajjadi, Z. Lotfi, Novel magnetic nanoparticles as adsorbent in ultrasound-assisted micro-solid-phase extraction for rapid pre-concentration of some trace heavy metal ions in environmental water samples: desirability function, Chem. Pap., 74 (2020) 1143–1159.
[15] Y.Y. Liang, L.M. Zhang, W. Li, R.F. Chen, Polysaccharide-modified iron oxide nanoparticles as an effective magnetic affinity adsorbent for bovine serum albumin, Colloid Polym. Sci., 285 (2007) 1193–1199.
[16] D.Z. Husein, R. Hassanien, M.F. Al-Hakkani, Green-synthesized copper nano-adsorbent for the removal of pharmaceutical pollutants from real wastewater samples, Heliyon, 5 (2019), doi: 10.1016/j.heliyon.2019.e02339.
[17] W.S. Hummers Jr., R.E. Offeman, Preparation of graphitic oxide, J. Am. Chem. Soc., 80 (1958) 1339–1339.
[18] D.C. Marcano, D.V. Kosynkin, J.M. Berlin, A Sinitskii, Z. Sun, A. Slesarev, Lawrence B. Alemany, Wei Lu, J.M. Tour, Improved synthesis of graphene oxide, ACS Nano, 4 (2010) 4806–4814.
[19] L.J. Cote, F. Kim, J. Huang, Langmuir − Blodgett assembly of graphite oxide single layers, J. Am. Chem. Soc., 131 (2008) 1043–1049.

[20] Y. Zhong, S. Wang, Y. He, G. Song, Synthesis of magnetic/graphene oxide composite and application for high-performance removal of polycyclic aromatic hydrocarbons from contaminated water, Nano Life, 5 (2015) 1542006, doi: 10.1142/S1793984415420064.
[21] R.L. Sarah Connors, E.V.E. Renee Lanza, A. Sirocki, Removal of Ibuprofen from Drinking Water Using Adsorption, BS Thesis, Worcester Polytechnic Institute, Worcester, MA, 2013.
[22] D.Z. Husein, Adsorption and removal of mercury ions from aqueous solution using raw and chemically modified Egyptian mandarin peel, Desal. Water Treat., 51 (2013) 6761–6769.
[23] P. Banerjee, P. Das, A. Zaman, P. Das, Application of graphene oxide nanoplatelets for adsorption of ibuprofen from aqueous solutions: evaluation of process kinetics and thermodynamics, Process Saf. Environ. Prot., 101 (2016) 45–53.
[24] L. Rafati, M. Ehrampoush, A. Rafati, M. Mokhtari, A. Mahvi, Removal of ibuprofen from aqueous solution by functionalized strong nano-clay composite adsorbent: kinetic and equilibrium isotherm studies, Int. J. Environ. Sci. Technol., 15 (2018) 513–524.
[25] G. Dönmez, Z. Aksu, Removal of chromium(VI) from saline wastewaters by *Dunaliella* species, Process Biochem., 38 (2002) 751–762.
[26] H.R. Nodeh, W.A.W. Ibrahim, I. Ali, M.M. Sanagi, Development of magnetic graphene oxide adsorbent for the removal and preconcentration of As(III) and As(V) species from environmental water samples, Environ. Sci. Pollut. Res., 23 (2016) 9759–9773.
[27] T. Gu, S.O. Rastegar, S.M. Mousavi, M. Li, M. Zhou, Advances in bioleaching for recovery of metals and bioremediation of fuel ash and sewage sludge, Bioresour. Technol., 261 (2018) 428–440.
[28] P. Chen, H. Song, L. Zhou, J. Chen, J. Liu, S. Yao, Magnetic solid-phase extraction based on ferroferric oxide nanoparticles doubly coated with chitosan and β-cyclodextrin in layer-by-layer mode for the separation of ibuprofen, RSC Adv., 6 (2016) 56240–56248.
[29] S. Rahdar, A. Rahdar, M. Khodadadi, S. Ahmadi, Error analysis of adsorption isotherm models for penicillin G onto magnesium oxide nanoparticles, Appl. Water Sci., 9 (2019) 190, doi: 10.1007/s13201-019-1060-3.
[30] S. Ahmadi, F. Kord Mostafapour, Adsorptive removal of aniline from aqueous solutions by *Pistacia atlantica* (Baneh) shells: isotherm and kinetic studies, J. Sci. Technol. Environ. Inform., 5 (2017) 327–335.
[31] D. Balarak, F.K. Mostafapour, A. Joghataei, Experimental and kinetic studies on penicillin G adsorption by Lemna minor, Br. J. Pharm. Res., 9 (2016) 1–10.
[32] M.N. Alnajrani, O.A. Alsager, Removal of antibiotics from water by polymer of intrinsic microporosity: isotherms, kinetics, thermodynamics, and adsorption mechanism, Sci. Rep., 10 (2020) 1–14.
[33] D.T.C. Nguyen, H.T.N. Le, T.S. Do, V.T. Pham, L. Dai Tran, V.T.T. Ho, T.V. Tran, D.C. Nguyen, T.D. Nguyen, L.G. Bach, H.K.P. Ha, V.T. Doan, Metal-organic framework MIL-53 (Fe) as an adsorbent for ibuprofen drug removal from aqueous solutions: response surface modeling and optimization, J. Chem., 2019 (2019) 1–11.
[34] H. Hossini, R.D.C. Soltani, M. Safari, A. Maleki, R. Rezaee, R. Ghanbari, The application of a natural chitosan/bone char composite in adsorbing textile dyes from water, Chem. Eng. Commun., 204 (2017) 1082–1093.
[35] A. Arab Markadeh, A. Rezaee, S. Rastegar, H. Hossini, S. Ahmadi, E. Hoseinzadeh, Optimization of Remazol Brilliant Blue adsorption process from aqueous solutions using multi-walled carbon nanotube, Desal. Water Treat., 57 (2016) 13357–13365.
[36] M. Masoudi, M. Mashreghi, E. Goharshadi, A. Meshkini, Multifunctional fluorescent titania nanoparticles: green preparation and applications as antibacterial and cancer theranostic agents, Artif. Cells Nanomed. Biotechnol., 46 (2018) 248–259.
[37] B.N. Bhadra, I. Ahmed, S. Kim, S.H. Jhung, Adsorptive removal of ibuprofen and diclofenac from water using metal-organic framework-derived porous carbon, Chem. Eng. J., 314 (2017) 50–58.
[38] H. Ge, J. Wang, Ear-like poly (acrylic acid)-activated carbon nanocomposite: a highly efficient adsorbent for removal of Cd(II) from aqueous solutions, Chemosphere, 169 (2017) 443–449.
[39] A. Pholosi, E.B. Naidoo, A.E. Ofomaja, Intraparticle diffusion of Cr(VI) through biomass and magnetite coated biomass: a comparative kinetic and diffusion study, S. Afr. J. Chem. Eng., 32 (2020) 39–55.
[40] H. Nourmoradi, A. Daneshfar, S. Mazloomi, J. Bagheri, S. Barati, Removal of Penicillin G from aqueous solutions by a cationic surfactant modified montmorillonite, MethodsX, 6 (2019) 1967–1973.
[41] S. Chavoshan, M. Khodadadi, N. Nasseh, A.H. Panahi, A. Hosseinnejad, Investigating the efficiency of single-walled and multi-walled carbon nanotubes in removal of penicillin G from aqueous solutions, Environ. Health Eng. Manage. J., 5 (2018) 187–196.
[42] N. Ayawei, A.N. Ebelegi, D. Wankasi, Modelling and interpretation of adsorption isotherms, J. Chem., 2017 (2017) 1–11.
[43] R.N. Coimbra, C. Escapa, M. Otero, Adsorption separation of analgesic pharmaceuticals from ultrapure and waste water: batch studies using a polymeric resin and an activated carbon, Polymers, 10 (2018) 958, doi: 10.3390/polym10090958.
[44] N. Cai, P. Larese-Casanova, Application of positively-charged ethylenediamine-functionalized graphene for the sorption of anionic organic contaminants from water, J. Environ. Chem. Eng., 4 (2016) 2941–2951.
[45] D. Balarak, F. Kord Mostafapour, A. Rakhsh Khorshid, Isotherm and kinetic study on the adsorption of penicillin g from aqueous solution by using modified canola, J. Rafsanjan Univ. Med. Sci., 15 (2016) 101–114.